A Prospective Evaluation of Chemokine Receptor-4 (CXCR4) Overexpression in High-grade Glioma Using ^{68}Ga-Pentixafor (Pars-Cixafor™) PET/CT Imaging

Habibollah Dadgar, Nasim Norouzbeigi, Majid Assadi, Esmail Jafari, Batool Al-Balooshi, Akram Al-Ibraheem, Abdulredha A. Esmail, Fahad Marafi, Mohamad Haidar, Haider Muhsin Al-Alawi, Yehia Omar, Sharjeel Usmani, Andrea Cimini, Maria Ricci, Hossein Arabi, Habib Zaidi, Ph.D

Background: While magnetic resonance imaging (MRI) remains the gold standard for morphological imaging, its ability to differentiate between tumor tissue and treatment-induced changes on the cellular level is insufficient. Notably, glioma cells, particularly glioblastoma multiforme (GBM), demonstrate overexpression of chemokine receptor-4 (CXCR4). This study aims to evaluate the feasibility of non-invasive ^{68}Ga-Cixafor™ PET/CT as a tool to improve diagnostic accuracy in patients with high-grade glioma.

Methods: In this retrospective analysis, a database of histopathology-confirmed glioma patients with MRI findings consistent with high-grade gliomas was utilized. Within 2 weeks of their MRI, these patients underwent ^{68}Ga-Cixafor™ PET/CT scans to assess CXCR4 expression. Both visual scoring based on established criteria and semi-quantitative measures including maximum standardized uptake value (SUV_{max}) and tumor-to-background ratios (TBR) were calculated to analyze the PET/CT data.

Results: Our retrospective study enrolled 29 histologically confirmed glioma patients with MRI findings consistent with high-grade gliomas. All patients underwent ^{68}Ga-Cixafor™ PET/CT scans within 2 weeks of their MRI, specifically at one-hour post-injection time point. Visual assessment based on a standardized scoring system identified 27 positive scans out of 29 (93.1%). Median SUV_{max} was 2.31 (range: 0.49–9.96) and median TBR was 20 (range: 6.12–124.5). Pathological analysis revealed 5 grade III (17.24%) and 24 grade IV (82.75%) lesions among the 29 patients. Notably, the median SUV_{max} of grade IV lesions (2.85) was significantly higher than grade III lesions (1.27) ($P = 0.02$). Conversely, there was no significant difference in median TBR between grade IV (20) and grade III (22.37). These findings support the correlation between high CXCR4 expression, particularly in high-grade gliomas, and elevated uptake of ^{68}Ga-Pentixafor. While areas with high uptake showed CXCR4 expression, areas with low uptake did not exhibit noticeable expression (data not shown).

Conclusion: This study demonstrated that ^{68}Ga-Cixafor™ PET exhibits a TBR with minimal cortical uptake, significantly enhancing glioma detection compared to conventional imaging methods. This, combined with the potential therapeutic capabilities of CXCR4-

Acad Radiol 2025; 32:2247–2256

From the Cancer Research Center, RAZAVI Hospital, Imam Reza International University, Mashhad, Iran (H.D., N.N.); The Persian Gulf Nuclear Medicine Research Center, Department of Molecular Imaging and Radionuclide Therapy (MIRT), Bushehr Medical University Hospital, Bushehr University of Medical Sciences, Bushehr, Iran (M.A., E.J.); Dubai Nuclear medicine & Molecular imaging Center, Dubai Academic Health corporation, DAHC, United Arab Emirates (B.A.B.); Department of Nuclear Medicine, King Hussein Cancer Center, Amman, Jordan (A.A.I.); Division of Nuclear Medicine/Department of Radiology and Nuclear Medicine, University of Jordan, Amman, Jordan (A.A.I.); Nuclear Medicine Department, Kuwait Cancer Control Center, Kuwait City, Kuwait (A.A.E.); Jaber Alahmad Center of Nuclear Medicine and Molecular Imaging, Kuwait City, Kuwait (F.M.); Diagnostic Clinical Radiology Department, American University of Beirut, Beirut, Lebanon (M.H.); Nuclear Medicine department, Amir Al-momineen Specialty Hospital, Al-Najaf Governorate, Iraq (H.M.A.A.); Middle Euphrates Cancer Hospital, Al-Najaf Governorate, Iraq (H.M.A.A.); PET-CT department at Misr Radiology Center, Heliopolis, Egypt (Y.O.); Department of Nuclear Medicine Sultan Qaboos Comprehensive Cancer Care and Research Center (SQCCCRC), Seeb, Oman (S.U.); Nuclear Medicine Unit, St. Salvatore Hospital, 67100 L'Aquila, Italy (A.C.); Nuclear Medicine Unit, Cardarelli Hospital, 86100 Campobasso, Italy (M.R.); Division of Nuclear Medicine and Molecular Imaging, Department of Medical Imaging, Geneva University Hospital, CH-1211 Geneva 4, Switzerland (H.A., H.Z.); Department of Nuclear Medicine and Molecular Imaging, University of Groningen, University Medical Center Groningen, 9700 RB Groningen, Netherlands (H.Z.); Department of Nuclear Medicine, University of Southern Denmark, Odense, Denmark (H.Z.); University Research and Innovation Center, Óbuda University, Budapest, Hungary (H.Z.). Received June 27, 2024; revised November 1, 2024; accepted November 25, 2024. **Address correspondence to:** H.Z. e-mail: habib.zaidi@hcuge.ch

https://doi.org/10.1016/j.acra.2024.11.064

targeting radiopharmaceuticals, highlights the promise of ^{68}Ga-Cixafor™ as a valuable tool for not only improved glioma diagnosis but also personalized treatment strategies.

Key Words: CXCR4; ^{68}Ga-Pentixafor; PET/CT; MRI; GBM.

INTRODUCTION

Primary brain tumors constitute approximately 2% of all tumor cases and are categorized into benign and malignant forms (1). The World Health Organization (WHO) classifies primary brain tumors using a grading scheme from I to IV, based on their histological aggressiveness: WHO grades III and IV gliomas are considered high-grade gliomas (HGG), which are the most fatal brain tumors (2). Glioblastoma multiforme (GBM) is classified as a WHO grade IV glioma (3) and represents the most aggressive form of cancer that can develop in the brain or spinal cord. GBM is often challenging to treat, and a cure is typically unattainable (4). Despite the combination of treatment modalities such as surgery, radiotherapy, and chemotherapy with temozolomide (TMZ), the 5-year survival rate remains low, typically around 5% (4, 5). Although the precise delineation of brain tumors remains a significant challenge, magnetic resonance imaging (MRI) is currently regarded as the gold standard for diagnosing brain tumors due to its superior soft tissue contrast and sensitivity.

In parallel, positron emission tomography (PET), akin to functional MRI (fMRI), is widely utilized to offer supplementary insights into brain activity. Various radiotracers have been explored for brain tumor imaging over the past few decades (6–12). However, PET scanners possess limited spatial resolution, impeding the detection of rapid changes in brain activation. Furthermore, while some of these tools exhibit greater specificity than MRI, they still lack the necessary specificity for tumor cells, rendering accurate diagnosis challenging (13). Consequently, the identification of new receptors or biomarkers holds potential for improving therapeutic approaches. The European Association of Neuro-Oncology, the European Association of Nuclear Medicine (EANM), and the Response Assessment in Neuro-Oncology Working Group have acknowledged the significant role of ^{18}F-Fluoroethyl-l-tyrosine (^{18}F-FET) PET in the early detection and assessment of postoperative/chemoradiotherapy response in glioma patients (14). When biopsy from the lesion is not feasible, ^{18}F-FET-PET imaging offers a potent approach to evaluating primary brain tumors, enabling differentiation between chemotherapy-related changes and tumor recurrence (8,15,16).

Chemokine receptor-4 (CXCR4), part of the G protein-coupled chemokine receptor family, plays a vital role in neoangiogenesis and inflammation (17,18,19). Moreover, CXCR4 is known to be overexpressed in various types of cancer, including ovarian, prostate, esophageal, and renal cell carcinoma (20,21). The study conducted by Rubin et al. explored the inhibitory effects of a small-molecule antagonist targeting CXCR4 on the intracranial growth of primary brain tumors in a xenograft animal model (22). Their findings strongly support the crucial role of CXCR4 in promoting glioma progression. Similarly, in a recent study by Yao et al., the ERK and PI3K/AKT signaling pathways mediated by CXCL12/CXCR4 were identified as potential targets for therapy in GBM (23). Furthermore, the CXCL12/CXCR4 axis has been implicated in tumorigenesis and disease progression, and its therapeutic applications, particularly in hematological malignancies, have been recognized (24,25).

Notably, CXCR4 expression and CXCL12 secretion are prevalent in hypoxic areas of the tumor, influencing angiogenesis and tumor progression (19,26). Hypothetically, the use of CXCR4 antagonists could disrupt the interaction between CXCR4 and CXCL12, presenting a valuable therapeutic option in GBM treatment. Building upon this premise, Fricker et al. investigated the CXCR4 antagonist, plerixafor, in a mouse model to inhibit tumor recurrence in GBM. Their study demonstrated that plerixafor effectively inhibits the binding of CXCL12 to CXCR4, resulting in GBM cell shrinkage and the prevention of tumor recurrence even after discontinuation of plerixafor exposure (27,28). The rationale behind this approach is to block the CXCL12/CXCR4 axis, which is responsible for tumor regeneration, progression, and metastasis. In phase I/II clinical trials, the combination of plerixafor and temozolomide (TMZ) was evaluated after radiation therapy in patients with HGG to determine the optimal treatment dosage at the early stage of diagnosis (29).

Recently, a radioactively labeled cyclic pentapeptide called ^{68}Ga-Pentixafor has been developed for PET imaging, exhibiting high affinity for CXCR4 receptors and low background activity in the brain cortex (30–34). Increased CXCR4 expression has been observed in higher-grade astrocytomas according to the WHO classification (35,36), and it has been correlated with poor prognosis in GBM patients (37–42). The theranostic compound ^{177}Lu-Pentixather has shown promising potential. Notably, one advantage of ^{68}Ga-Pentixafor/^{177}Lu-Pentixather over ^{68}Ga/^{177}Lu-PSMA is its presence in the neovasculature of various tumor types (43), as CXCR4 is found not only on the neovasculature but also on tumor cells. A recent investigation by Lapa et al. reported promising results with ^{68}Ga-Pentixafor PET in 11 out of 13 GBM patients (44). Although the sample size was small, these

findings have provided encouragement to further examine CXCR4 expression in a larger population of high-grade gliomas. Upon thorough examination of the findings from both studies, it is evident that ^{68}Ga-Pentixafor/^{177}Lu-Pentixather demonstrates a superior efficacy in targeting the neovasculature of diverse tumor types when compared to ^{68}Ga/^{177}Lu-PSMA.

In this retrospective analysis, we utilized a database of histopathology-confirmed glioma patients with MRI findings consistent with high-grade gliomas to assess the feasibility of non-invasive ^{68}Ga-Cixafor™ PET/CT in enhancing diagnostic accuracy for glioma cells.

MATERIALS AND METHODS

Participants

From August 2020 to July 2022, our center received 29 glioma patients with confirmed histopathology and positive MRI findings for evaluation of CXCR4 expression using ^{68}Ga-Cixafor™ PET/CT. This retrospective study encompassed patients with various types of high-grade gliomas (HGG), including GBM, Anaplastic Astrocytoma, and Anaplastic Oligodendroglioma. Alongside PET/CT, all patients also underwent MRI scans, with a maximum interval of three weeks between PET and MRI examinations. All assessments were conducted in accordance with the principles outlined in the Helsinki Declaration and national regulations. The retrospective analysis adhered to the ethical guidelines of our university's ethics commission, and the requirement for individual informed consent for this analysis was waived.

^{68}Ga-Cixafor™ PET/CT Data Acquisition

Radiopharmaceutical Production

The radiolabeling process of ^{68}Ga-Pentixafor was conducted using a fully automated labeling module from SCINTOMICS GmbH, adhering to Good Manufacturing Practice (GMP) regulations. Initially, ^{68}Ga radioisotope was eluted with 0.1 M HCl from a PARS-GalluGEN ^{68}Ge/^{68}Ga generator and utilized in the labeling procedure. Subsequently, the radioactivity was transferred to a strong cation exchange (SCX) cartridge, where ^{68}Ga was eluted with NaCl (1.7 mL, 5 M) and then transferred to a borosilicate vial containing 25 μg Pentixafor and HEPES (3 mL, 1.5 M) serving as a buffer. The reaction mixture underwent heating at 125 °C for 6 min, followed by cooling and passage through a preconditioned C-18 cartridge. The cartridge was washed three times with water and eluted with a solution of 2 mL EtOH/H2O (50/50) to yield the ^{68}Ga-Pentixafor. The pH was subsequently adjusted by adding 20 mL phosphate buffer saline (PBS). Prior to clinical use, the final product underwent sterilization using a 0.22 μ Millex-LG filter (EMD Millipore). The ^{68}Ga-Pentixafor utilized in this study exhibited high radiochemical purity (> 98%), radionuclide purity (> 99%), endotoxin level (< 175 EU/mL), and maintained a pH within the range of 5–8.5, as characterized.

Following synthesis, the product vial is extracted from the Modular Lab Pharm Tracer (MLPT) module and subjected to comprehensive quality control assessments, including the evaluation of various parameters. These assessments encompass the determination of total product activity, confirmation of ^{68}Ga 3+identity via half-life measurement, determination of chemical purity (including pH, sterility, and endotoxin levels), and assessment of radiochemical purity using high-pressure liquid chromatography (HPLC). The stability of the product at room temperature is monitored using radio-HPLC over a 4-hour period, employing a standardized method with water + 0.1% trifluoroacetic acid (TFA) as mobile phase A and acetonitrile + 0.1% TFA as mobile phase B. This is followed by a gradient of 0–25 min with 0–100% of mobile phase A and 25–28 min with a transition from 100% to 0% of mobile phase A. The limit of detection for radio-HPLC is 10 kBq/20 μL injected volume, with an approximate recovery rate of 80%. Additionally, iTLC analysis is conducted using a mobile phase consisting of ammonium acetate/methanol (1/1) and iTLC-SG strips as stationary phase. This further ensures the quality and stability of the synthesized product.

PET/CT Data Acquisition

The acquisition protocol involved the intravenous administration of ^{68}Ga-Pentixafor radiotracer to patients, with injected activity ranging from 114.7 to 193.5 MBq (mean: 154 ± 21 MBq). Imaging was performed on a PET/CT scanner (Biograph 6 TrueV, SIEMENS Healthcare, Erlangen, Germany), which incorporated a 6-slice spiral CT component. The PET axial-field-of-view encompassed 21.6 cm, allowing the entire skull to be accommodated within a single bed position. Data acquisition employed a time-based method, with each bed position scanned for 10 min, commencing 60 min post-intravenous injection. Moreover, three patients underwent 30 min post-injection imaging. The objective was to investigate differences in radiotracer uptake at various scan times. This investigation may provide insights into the optimal imaging time for ^{68}Ga-Pentixafor PET imaging in patients with high-grade gliomas, potentially reducing the waiting period while maximizing uptake in the affected lesions. Diagnostic CT scans of the brain were acquired preceding PET scans to facilitate lesion localization, attenuation, and scatter corrections. CT scan parameters included 240 mAs, 130 kV, a matrix size of 512 × 512, 3 mm slice thickness, reconstruction increment of 1.5 mm, a rotation time of 1 s, and a pitch of 0.55. PET images were reconstructed using the Ordered Subset - Expectation Maximization (OSEM) algorithm with 21 subsets, 2 iterations and Gaussian filtering with 5 mm full-width half-maximum (FWHM) at 60 min post-injection.

For semi-quantitative analysis, an axial image slice was selected through a volume of interest (VOI) encompassing the tumor lesion and its border. A circular area of interest

(ROI) with a diameter of 1 cm was placed in the region of highest activity to determine the tumor's SUV_{max}. Additionally, a 2.5 cm ROI was positioned in the contralateral hemisphere at the level of the semi-oval center to calculate the tumor-to-background ratio (TBR). Two neuroradiology fellowship-trained physicians with more than 8 years of experience analyzed the PET/CT data, with all image interpreters blinded to the patients' data.

MRI Acquisition

MRI was conducted using a 1.5 Tesla scanner (Sonata, Siemens-Erlangen, Germany). T2-weighted and fast-spin echo sequences (660 ms/100–110 ms, 2 mm slice thickness, 320 × 240 matrices), fluid-attenuated inversion recovery (FLAIR) sequence, and T1-weighted gradient-echo sequences (TR = 1860 ms, TE = 4.38 ms with 1.2 mm slice thickness, 256 × 192 matrices) were acquired both before and after gadolinium administration. Two neuroradiology fellowship-trained physicians with more than 8 years of experiences analyzed MRI based on the Response Assessment in Neuro-Oncology (RANO) criteria during a consensus reading to evaluate potential recurrence (45). The T2 SPACE dark fluid sequence, characterized by a TR of 660 ms and TE ranging from 100 to 110 ms, yields enhanced imaging of abnormal structures, such as tumors, by providing more detailed slices. This technique offers excellent spatial resolution, which is crucial for evaluating these structures, as it enables the identification of abnormal signal intensities and aids in the detection of various abnormalities. Consequently, it can be asserted that the T2 SPACE dark fluid sequence plays a vital and highly informative role in the diagnostic process. A standardized field-of-view (FOV) of 230 mm was employed in this imaging protocol.

Statistical Analysis

All statistical analyses were performed using SPSS software version 21. Descriptive statistics were calculated for each variable. Categorical variables were presented in terms of percentage and frequency as deemed appropriate. The Mann-Whitney U test was employed to compare continuous groups. A p-value less than 0.05 was regarded as statistically significant. The final determination of recurrence was based on histopathology when accessible. For patients where histopathology was not available, recurrence was determined based on follow-up clinical and/or imaging data. Tumor progression clinically or on imaging was designated as recurrence.

RESULTS

In our cohort, a total of 29 cases were enrolled, consisting of 13 females (45%) and 16 males (55%). The median age of the patients was 56 years old, ranging from 11 to 73. The distribution of tumor types included 23 cases of GBM, two cases of astrocytoma, three cases of oligodendroglioma, and one case of gliosarcoma. Among the 29 cases, 24 were referred for initial staging, while five were referred for recurrence assessment. Among the five cases referred for recurrence assessment, all had a history of surgery, four had a history of chemotherapy, and one had a history of radiotherapy. The characteristics of the patients are presented in Table 1.

Regarding tumor location, 8 patients had frontotemporal lesions (27%), 5 had temporal lesions (17%), 7 had parietal (parieto-occipital) tumors (24%), 5 had frontoparietal lesions (17%), 2 had temporoparietal lesions (6.8%), and the remaining 2 had lesions in the parafalcine and diencephalic region (6.8%).

Out of the 29 cases, 27 showed positive PET/CT scan results, with a median SUV_{max} of 2.31 (ranging from 0.49 to 9.96) and a TBR of 20 (ranging from 6.12 to 124.5). The median SUV_{max} of WHO grade IV lesions was significantly higher than that of grade III lesions (2.68 [0.83–9.96] vs. 1.51 [0.49–2.05]) ($P = 0.02$). However, there was no significant difference between grade IV (20 [8.36–124.5]) and grade III (22.37 [6.12–51.25]) in terms of median TBR.

These findings validate the correlation between high expression of CXCR4, particularly in high-grade gliomas, and elevated uptake of ^{68}Ga-Pentixafor. Conversely, areas within the same tumor lacking noticeable uptake of ^{68}Ga-Pentixafor exhibited either minimal or no expression of the receptor (not demonstrated in this work) (46,47).

TABLE 1. Summary of Patient Characteristics

Sex	
Male	16 (55%)
Female	13 (45%)
Age (year)	
Median	56
Range	11–73
Tumor type (WHO classification)	
Glioblastoma (GBM)	23 (79%)
Astrocytoma	2 (7%)
Oligodendroglioma	3 (10%)
Gliosarcoma	1 (4%)
Study (Referral investigation)	
Staging	24 (83%)
Recurrence	5 (17%)
Prior treatment interventions	
Surgery*	5 (100%)
Chemotherapy	4 (80%)
Radiotherapy	1 (20%)
SUVmax (Semi-quantitative analysis)	
Median	2.31
Range	0.49–9.96
TBR	
Median	20
Range	6.12–124.5

*Only patients referred for recurrence were expressed.

TABLE 2. Characteristics of Patients (16 Males, 13 Females) with Grade 3, 4 Gliomas Included in this Study

Diagnosis based on histology	SUV_{max} of lesions	Age/sex	P number	TBR_{max}
GBM	4.09	53/F	1	10.77
GBM	2.23	55/M	2	74.3
GBM	3.14	51/M	3	13.08
Anaplastic Astrocytoma (WHO III)	2.05	31/F	4	51.25
GBM	-	11/F	5	-
GBM	1.98	60/M	6	24.75
GBM	1.87	62/M	7	23.37
GBM	2.31	73/M	8	10.04
GBM	1.48	64/F	9	16.4
Anaplastic oligoglioma (WHO III)	-	56/F	10	-
GBM	3.01	58/F	11	11.14
Anaplastic Oligodendroglioma (WHO III) or Glioblastoma (WHO IV)	5.75	55/F	12	13.7
GBM	6.36	32/M	13	8.36
Anaplastic Oligodendroglioma (WHO III)	1.68	33/F	14	28
GBM	2.31	50/M	15	25.6
GBM	3.67	68/M	16	12.7
GBM	2.8	56/M	17	40
Anaplastic Oligodendroglioma (WHO III) or Glioblastoma (WHO IV)	0.49	63/F	18	6.12
GBM	2.68	33/M	19	29.7
GBM	3.56	65/F	20	11.12
GBM	4.91	59/F	21	10.67
Gliosarcoma	2.50	56/M	22	41.6
Anaplastic Astrocytoma (WHO III)	1.34	62/M	23	16.75
GBM	5.02	55/F	24	62.7
GBM	0.83	38/M	25	13.83
GBM	1.30	62/M	26	26
GBM	1.69	63/M	27	21.12
GBM	1.2	46/M	28	20
GBM	9.96	63/F	29	124.5

(F; Female, M; Male, GBM; Glioblastoma Multiform, TBR; Tumor to background ratio)

Figures 1–3 depict examples of CXCR4 expression in glioma cells. Figure 1 illustrates a 63-year-old female with a history of GBM suspected of recurrence post-surgery and chemotherapy. Both ^{68}Ga-Cixafor™ PET/CT and MRI were conducted, with MRI taken two weeks prior to the PET scan. The ^{68}Ga-Cixafor™ PET/CT, alongside T1-weighted (T1W) and T2-weighted (T2W) MRI images, revealed a lesion in the right occipito-parietal region with SUV_{max} of 9.96. In contrast, the contralateral site exhibited an SUV_{max} of 0.08. This case highlights a high level of agreement between MRI and ^{68}Ga-Pentixafor PET/CT imaging for GBM.

Figure 2 depicts a 56-year-old male presenting with recent-onset headaches and diagnosed with Gliosarcoma. The patient underwent ^{68}Ga-Cixafor™ PET/CT imaging two weeks after undergoing MR imaging utilizing various protocols including FLAIR, T2-weighted, Dark Fluid, and T1-weighted. The PET/CT scan revealed an SUV_{max} of 2.5 in the right frontoparietal lesion, while the contralateral site exhibited an SUV_{max} of 0.06. Notably, there is a correlation observed between the MRI lesions captured using various sequences and the uptake of ^{68}Ga-Pentixafor in PET/CT imaging.

The case in Figure 3 depicts a 32-year-old male with recent-onset headaches diagnosed with GBM and a large right fronto-temporal mass based on MRI findings. The patient underwent a subsequent referral for a ^{68}Ga-Cixafor™ PET/CT scan, with MRI conducted one week prior to the PET/CT scan utilizing various sequences, including Dark Fluid, FLAIR, T1-weighted, and T2-weighted imaging. The ^{68}Ga-Cixafor™ PET/CT scan, performed 30 min post-injection, revealed an SUV_{max} of 5.53 in the lesion. Furthermore, the scan conducted one-hour post-injection demonstrated an SUV_{max} of 6.36 in the lesion, with the contralateral site exhibiting an SUV_{max} of 0.76. Based on the SUV_{max} values, the imaging conducted one-hour post-injection of ^{68}Ga-Pentixafor appears to offer a superior TBR for GBM in comparison to the early imaging time point. Consequently, we recommend performing ^{68}Ga-Pentixafor PET/CT imaging at the one-hour post-injection time point for optimal results.

DISCUSSION

We investigated the expression of CXCR4 using ^{68}Ga-Cixafor™ PET/CT in glioma, where the majority of cases

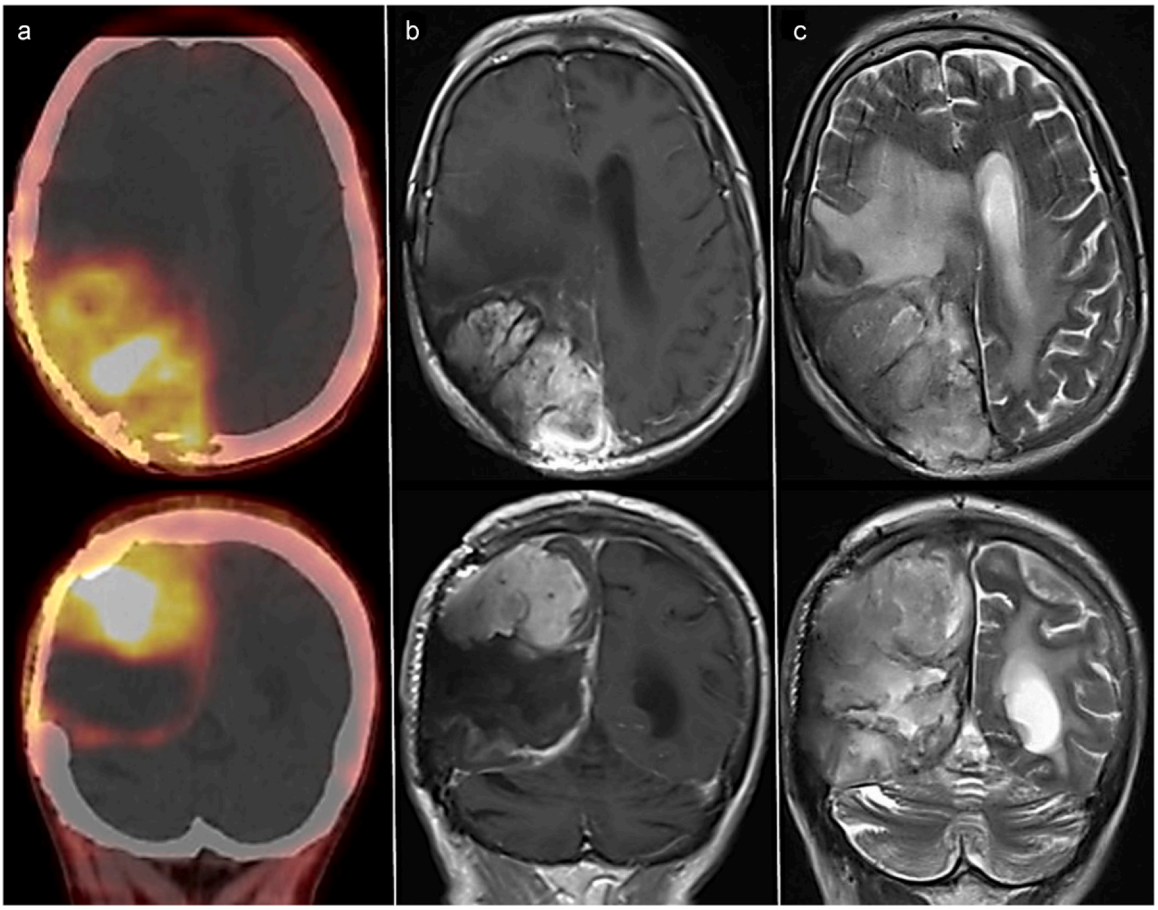

Figure 1. A 63-year-old female with a history of GBM suspected to recurrence after surgery and chemotherapy underwent ^{68}Ga-Cixafor™ PET/CT and MRI. MRI was performed two weeks prior to the PET scan. According to ^{68}Ga-Cixafor™ PET/CT **(a)**, T1-weighted (T1W) **(b)** and T2-weighted (T2W) images **(c)**, a lesion was observed in the right occipito-parietal region with SUV_{max} of 9.96. In contrast, the contralateral site showed an SUV_{max} of 0.08.

showed positive PET/CT results (27 out of 29 cases). The median SUV_{max} of WHO grade IV lesions was significantly higher than that of grade III lesions. This aligns with previous research indicating that CXCR4 expression in glioma cells correlates with higher tumor grade, recurrence, and poor prognosis (48,49). Given the pivotal role of CXCR4 receptors in glioma tumor cell progression and metastasis, they have emerged as promising targets for treatment modalities. Therefore, non-invasive imaging of CXCR4 targets using PET/CT can be valuable for early-stage diagnosis and recurrence assessment following surgery or chemoradiotherapy.

To support our findings, Jacobs et al. demonstrated a significant relationship between CXCR4 expression and glioma cell grade in a large cohort (50). They found CXCR4 overexpression in high-grade gliomas, particularly glioblastomas, while normal brain tissue showed no CXCR4 uptake. However, the results of Komatani et al.'s study contrasted with these findings, as they observed CXCR4 expression in all glioblastomas (24/24), anaplastic astrocytomas (9/9), and astrocytomas or oligoastrocytomas (10/11) (51). Similarly, Stevenson et al. reported CXCR4 expression in all cases of glioblastoma, albeit with a small sample size of five patients (40). Jacobs et al. utilized novel ^{68}Ga-Pentixafor PET imaging to examine CXCR4 expression in seven patients. Among them, five patients exhibited low/moderate ^{68}Ga-Pentixafor uptake, and all patients demonstrated significant tumor variation in CXCR4 staining. The authors suggested that discrepancies between CXCR4 staining and ^{68}Ga-Pentixafor uptake in malignant glioma cells could be attributed to variations in CXCR4 antibodies and different chemical structures of ^{68}Ga-Pentixafor used for staining.

Our findings are consistent with a prospective study conducted by Wang et al., who used ^{68}Ga-NOTA-NFB-PET to visualize CXCR4 expression in glioma patients (52). Interestingly, in our cohort, patients with WHO grade III gliomas exhibited minimal ^{68}Ga-Cixafor™ uptake. The discrepancy could potentially be attributed to receptor kinetics, internalization, and CXCR4 expression on the cell surface of glioma cells. However, further investigation is needed to confirm this hypothesis in a larger population encompassing different WHO grades of glioma.

The presence of Ki67 protein (pKi67) correlates with the proliferative activity of intrinsic cell populations within malignant

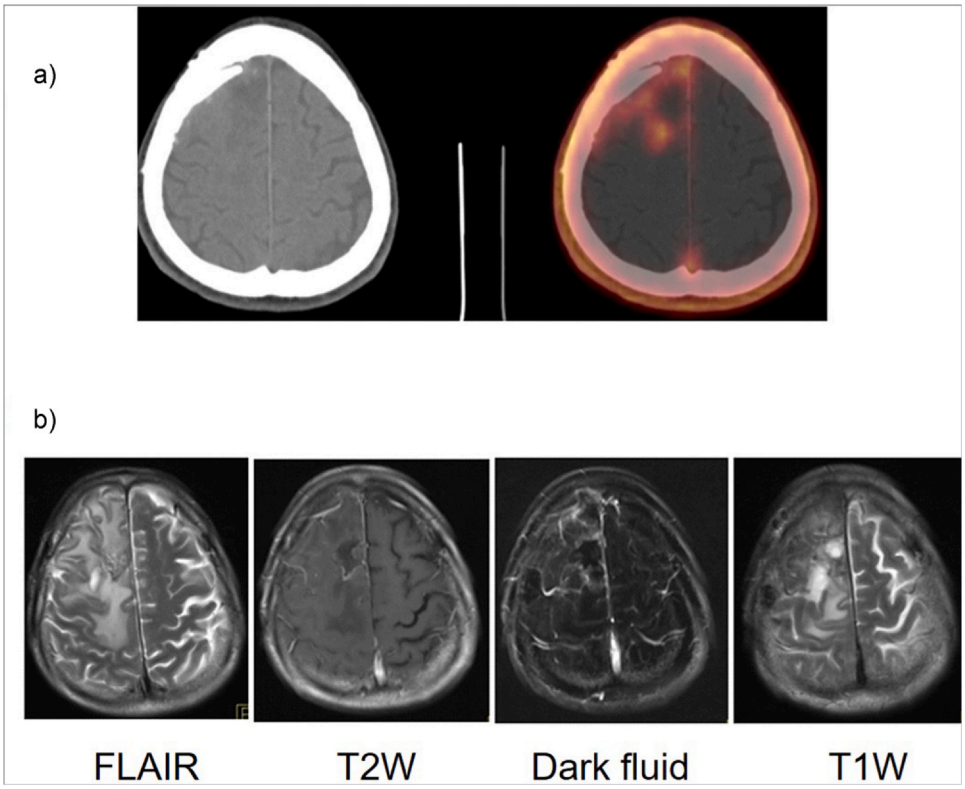

Figure 2. A 56-year-old male presenting with recent-onset headache, diagnosed as a Gliosarcoma case, underwent ^{68}Ga-Cixafor™ PET/CT **(a)** two weeks after MR imaging using different protocols (from left to right; FLAIR, T2W, Dark Fluid, and T1W) **(b)**. The right frontoparietal lesion exhibited an SUV_{max} of 2.5 (contralateral site SUV_{max} = 0.06).

tumors, thereby serving as an indicator of tumor aggressiveness. While Kaemmerer et al. highlighted a correlation between Ki-67 and CXCR4 expression in their examination of somatostatin and CXCR4 chemokine receptors in neuroendocrine neoplasms across different malignancies (53). Unfortunately, we were not able to compare our results with them due to the lack of data about Ki-67 for our patients. This issue was one of our study's limitations. In cases where CXCR4 immunostaining of patients was negative, ^{68}Ga-Pentixafor PET imaging can be utilized for CXCR4-PET-guided therapy. The use of ^{90}Y/^{177}Lu-labeled CXCR4 receptors as endoradiotherapy could hold promise as a treatment approach for glioblastoma patients. Preclinical studies have already shown that the first CXCR4 antagonist, plerixafor, reduced GBM stem cell survival, emphasizing the urgent need for the development of CXCR4 inhibitors as anti-GBM agents (24). Moreover, the CXCR4 antagonist PRX177561 has recently shown potential in suppressing GBM progression and enhancing the effects of antitumor chemoradiotherapy (54). Additionally, Bianco et al. reported lower expression of CXCR4 in GBM cells in 86 glioblastoma specimens, fewer than the number of cases analyzed by Jacobs et al. in their study (55). In clinical practice, ^{68}Ga-Pentixafor PET imaging has the potential to complement tumor imaging and treatment planning after surgery or radiotherapy, particularly in cases where CXCR4 is expressed. Demmer and Herrmann et al. developed dimeric peptides that target the chemokine receptor CXCR4 and utilized them in patients with advanced multiple myeloma (MM) (30,31,56). CXCR4-directed therapy, either alone or in combination with TMZ, has demonstrated promising results for glioblastoma treatment (57–59).

The primary objective of employing ^{68}Ga-Pentixafor is not only for tumor delineation but also to identify suitable candidates for CXCR4-targeted therapy. Considering the high expression of CXCR4 observed in pathological findings after tumor resection, the remaining or recurrent lesions could be potential candidates for treatment with ^{177}Lu-Pentixather. Moreover, the absence of ^{68}Ga-Pentixafor uptake at the tumor site does not necessarily imply the absence of a lesion. However, it does indicate that the case in question would not benefit from radionuclide therapy. Lapa et al. conducted a comprehensive study revealing similar discrepancies between ^{68}Ga-Pentixafor uptake and immunohistochemistry, which correlated with receptor kinetics and internalization (44). Additionally, physiological variations in the blood-brain barrier (BBB) among patients may contribute to the variability of ^{68}Ga-Pentixafor uptake in glioma tumor cells. Considering the crucial role of CXCR4 in angiogenesis, it would be valuable to monitor its expression in blood vessels using tumor molecular markers. As CXCR4 is overexpressed in tumor cells, adjunctive imaging with ^{68}Ga-Pentixafor can be performed to aid in radionuclide therapy with ^{177}Lu-Pentixather, thereby improving patient survival rates.

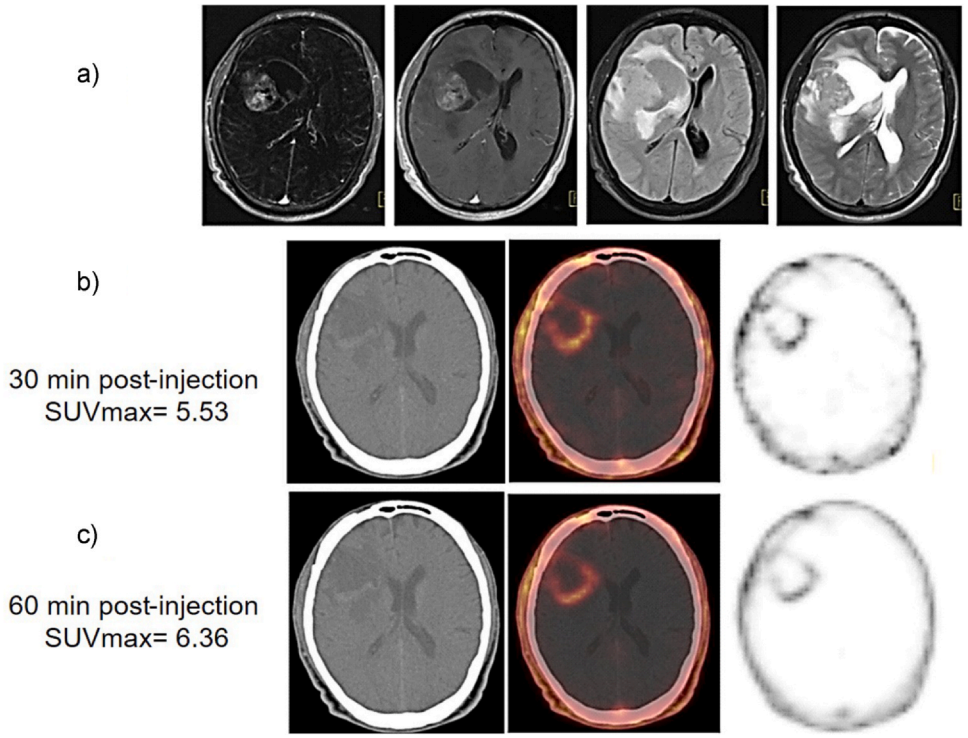

Figure 3. A 32-year-old male presenting with recent-onset headache, diagnosed with GBM and a large right fronto-temporal mass according to MRI **(a)**, referred for ^{68}Ga-Cixafor™ PET/CT scan. **(a)** MRI with different sequences (from left to right; Dark Fluid, Flair, T1W, T2W) was performed one week prior to the PET/CT scan. **(b)** ^{68}Ga-Cixafor™ PET/CT scan 30 min post-injection, showing an SUV_{max} of 5.53 in the lesion. **(c)** ^{68}Ga-Cixafor™ PET/CT scan after one-hour post-injection, revealing an SUV_{max} of 6.36 in the lesion (contralateral site SUV_{max} = 0.76).

Limitations of the Study

In the context of ^{68}Ga-Cixafor™ PET imaging, a retrospective study may lack standardized protocols for data collection, patient selection, and follow-up, which can result in incomplete or inconsistent data. Additionally, the absence of a prospective study design may limit the ability to establish causal relationships and draw definitive conclusions about the effectiveness or safety of ^{68}Ga-Cixafor™ imaging in specific clinical scenarios. Prospective studies with well-defined protocols and larger sample sizes are needed to validate the findings of retrospective studies and provide more robust evidence regarding the utility and reliability of ^{68}Ga-Cixafor™ PET imaging in clinical practice.

A small sample size can indeed impact the reliability of outcomes, limiting the ability to draw robust conclusions about the diagnostic or prognostic value of this imaging modality. Moreover, rare adverse events or less common outcomes may go unnoticed due to the limited number of participants, potentially underestimating potential risks or benefits. It is important to note that these limitations do not invalidate the value of retrospective studies or studies with small sample sizes. Such studies can provide valuable preliminary data, generate hypotheses for future research, and offer insights into novel applications of ^{68}Ga-Cixafor™ imaging. However, researchers and readers should interpret the findings with caution, acknowledging the inherent limitations and the need for further validation through larger, prospective studies to establish the full potential and limitations of ^{68}Ga-Cixafor™ imaging in various clinical scenarios.

Isocitrate dehydrogenase (IDH) mutation status and other relevant factors, such as O(6)-methylguanine-DNA methyltransferase (MGMT) promoter methylation, were not considered in our study. These factors have the potential to influence the efficacy of CXCR4-targeted therapies and should be investigated in future studies to gain a more comprehensive understanding of their role in tumor management. Acknowledging these limitations is crucial for ensuring a balanced interpretation of the study findings and for guiding future research efforts aimed at addressing these gaps in knowledge.

CONCLUSION

The uptake of ^{68}Ga-Cixafor™ in glioma cells suggests its potential as a valuable tool for assessing CXCR4 expression. Utilizing ^{68}Ga-Cixafor™ PET/CT could be beneficial for evaluating CXCR4 expression and identifying patients who would benefit from ^{177}Lu-Pentixather therapy. This finding emphasizes the potential of ^{68}Ga-Cixafor™ PET/CT as a useful strategy for patient selection and personalized

treatment in neuro-oncology. Such targeted imaging approaches hold promise for optimizing therapeutic interventions and improving outcomes for patients with glioma.

DECLARATION OF COMPETING INTEREST

The authors declare that they have no known competing financial interests or personal relationships that could have appeared to influence the work reported in this paper.

ACKNOWLEDGMENTS

This work was supported by the Swiss National Science Foundation under grant SNSF 320030_231742.

DISCLOSURE

The authors declare that they have no conflict of interest.

REFERENCES

1. Cimini A, Ricci M, Russo F, et al. Peptide receptor radionuclide therapy and primary brain tumors: an overview. Pharmaceuticals 2021; 14:872. https://doi.org/10.3390/ph14090872
2. Frosina G. Recapitulating the key advances in the diagnosis and prognosis of high-grade gliomas: second half of 2021 update. Int J Mol Sci 2023; 24:6375. https://doi.org/10.3390/ijms24076375
3. Skalli O, Wilhelmsson U, Orndahl C, et al. Astrocytoma grade IV (glioblastoma multiforme) displays 3 subtypes with unique expression profiles of intermediate filament proteins. Hum Pathol 2013; 44:2081–2088. https://doi.org/10.1016/j.humpath.2013.03.013
4. Ostrom QT, Gittleman H, Farah P, et al. CBTRUS statistical report: primary brain and central nervous system tumors diagnosed in the United States in 2006-2010. Neuro Oncol 2013; 15(2):ii1–ii56. https://doi.org/10.1093/neuonc/not151
5. Stupp R, Mason WP, van den Bent MJ, et al. Radiotherapy plus concomitant and adjuvant temozolomide for glioblastoma. N Engl J Med 2005; 352:987–996. https://doi.org/10.1056/NEJMoa043330
6. Galldiks N, Lohmann P, Albert NL, et al. Current status of PET imaging in neuro-oncology. Neurooncol Adv 2019; 1:vdz010. https://doi.org/10.1093/noajnl/vdz010
7. Assadi M, Nemati R, Shooli H, et al. An aggressive functioning pituitary adenoma treated with peptide receptor radionuclide therapy. Eur J Nucl Med Mol Imaging 2020; 47:1015–1016. https://doi.org/10.1007/s00259-019-04578-z
8. Dadgar H, Vafaee MS, Khorasanchi A, et al. Initial experience of (18) F-FET PET-MR image fusion for evaluation of recurrent primary brain tumors. World J Nucl Med 2023; 22:183–190. https://doi.org/10.1055/s-0043-1771282
9. Nemati R, Shooli H, Rekabpour SJ, et al. Feasibility and therapeutic potential of peptide receptor radionuclide therapy for high-grade gliomas. Clin Nucl Med 2021; 46:389–395. https://doi.org/10.1097/RLU.0000000000003599
10. Shooli H, Dadgar H, Wang YJ, et al. An update on PET-based molecular imaging in neuro-oncology: challenges and implementation for a precision medicine approach in cancer care. Quant Imaging Med Surg 2019; 9:1597–1610. https://doi.org/10.21037/qims.2019.08.16
11. Shooli H, Nemati R, Ahmadzadehfar H, et al. Theranostics in brain tumors. PET Clin 2021; 16:397–418. https://doi.org/10.1016/j.cpet.2021.03.005
12. Dadgar H, Norouzbeigi N, Jafari E, et al. Exploring the efficacy of FAPI PET/CT in the diagnosis and treatment management of colorectal cancer: a comprehensive literature review and initial experience. Clin Transl Imaging 2024; 12:235–252. https://doi.org/10.1007/s40336-023-00609-w
13. Hutterer M, Nowosielski M, Putzer D, et al. [18F]-fluoro-ethyl-L-tyrosine PET: a valuable diagnostic tool in neuro-oncology, but not all that glitters is glioma. Neuro-oncology 2013; 15:341–351. https://doi.org/10.1093/neuonc/nos300
14. Lundemann M, Munck Af Rosenschold P, Muhic A, et al. Feasibility of multi-parametric PET and MRI for prediction of tumour recurrence in patients with glioblastoma. Eur J Nucl Med Mol Imaging 2019; 46:603–613. https://doi.org/10.1007/s00259-018-4180-3
15. Filss CP, Albert NL, Boning G, et al. O-(2-[(18)F]fluoroethyl)-L-tyrosine PET in gliomas: influence of data processing in different centres. EJNMMI Res 2017; 7:64. https://doi.org/10.1186/s13550-017-0316-x
16. Vees H, Senthamizhchelvan S, Miralbell R, et al. Assessment of various strategies for 18F-FET PET-guided delineation of target volumes in high-grade glioma patients. Eur J Nucl Med Mol Imaging 2009; 36:182–193.
17. Zlotnik A, Burkhardt AM, Homey B. Homeostatic chemokine receptors and organ-specific metastasis. Nat Rev Immunol 2011; 11:597–606. https://doi.org/10.1038/nri3049
18. Jacobson O, Weiss ID. CXCR4 chemokine receptor overview: biology, pathology and applications in imaging and therapy. Theranostics 2013; 3:1–2. https://doi.org/10.7150/thno.5760
19. Furnari FB, Fenton T, Bachoo RM, et al. Malignant astrocytic glioma: genetics, biology, and paths to treatment. Genes Dev 2007; 21:2683–2710. https://doi.org/10.1101/gad.1596707
20. Zhao H, Guo L, Zhao H, et al. CXCR4 over-expression and survival in cancer: a system review and meta-analysis. Oncotarget 2015; 6:5022–5040. https://doi.org/10.18632/oncotarget.3217
21. Domanska UM, Kruizinga RC, Nagengast WB, et al. A review on CXCR4/CXCL12 axis in oncology: no place to hide. Eur J Cancer 2013; 49:219–230. https://doi.org/10.1016/j.ejca.2012.05.005
22. Rubin JB, Kung AL, Klein RS, et al. A small-molecule antagonist of CXCR4 inhibits intracranial growth of primary brain tumors. Proc Natl Acad Sci U S A 2003; 100:13513–13518. https://doi.org/10.1073/pnas.2235846100
23. Yao C, Li P, Song H, et al. RETRACTED ARTICLE: CXCL12/CXCR4 Axis upregulates twist to induce EMT in human glioblastoma. Mol Neurobiol 2016; 53:3948–3953.
24. Uy GL, Rettig MP, Motabi IH, et al. A phase 1/2 study of chemosensitization with the CXCR4 antagonist plerixafor in relapsed or refractory acute myeloid leukemia. Blood 2012; 119:3917–3924. https://doi.org/10.1182/blood-2011-10-383406
25. Kuhne MR, Mulvey T, Belanger B, et al. A fully human anti-CXCR4 antibody induces apoptosis in vitro and shows antitumor activity in vivo in hematologic malignancies. Am Assoc Cancer Res 2013; 19:357–366.
26. Wurth R, Bajetto A, Harrison JK, et al. CXCL12 modulation of CXCR4 and CXCR7 activity in human glioblastoma stem-like cells and regulation of the tumor microenvironment. Front Cell Neurosci 2014; 8:144. https://doi.org/10.3389/fncel.2014.00144
27. Fricker SP. Physiology and pharmacology of plerixafor. Transfus Med Hemother 2013; 40:237–245. https://doi.org/10.1159/000354132
28. Rios A, Hsu SH, Blanco A, et al. Durable response of glioblastoma to adjuvant therapy consisting of temozolomide and a weekly dose of AMD3100 (plerixafor), a CXCR4 inhibitor, together with lapatinib, metformin and niacinamide. Oncoscience 2016; 3:156–163. https://doi.org/10.18632/oncoscience.311
29. Thomas RP, Nagpal S, Iv M, et al. A phase I study of chemo-radiotherapy with plerixafor for newly diagnosed glioblastoma (GB). Am Soc Clin Oncol 2016; 34:2068.
30. Demmer O, Gourni E, Schumacher U, et al. PET imaging of CXCR4 receptors in cancer by a new optimized ligand. ChemMedChem 2011; 6:1789–1791. https://doi.org/10.1002/cmdc.201100320
31. Herrmann K, Lapa C, Wester HJ, et al. Biodistribution and radiation dosimetry for the chemokine receptor CXCR4-targeting probe 68Ga-pentixafor. J Nucl Med 2015; 56:410–416. https://doi.org/10.2967/jnumed.114.151647
32. Gourni E, Demmer O, Schottelius M, et al. PET of CXCR4 expression by a 68Ga-labeled highly specific targeted contrast agent. J Nucl Med 2011; 52:1803–1810.
33. Philipp-Abbrederis K, Herrmann K, Knop S, et al. In vivo molecular imaging of chemokine receptor CXCR 4 expression in patients with advanced multiple myeloma. EMBO Mol Med 2015; 7:477–487. https://doi.org/10.15252/emmm.201404698
34. Wester HJ, Keller U, Schottelius M, et al. Disclosing the CXCR4 expression in lymphoproliferative diseases by targeted molecular imaging. Theranostics 2015; 5:618–630. https://doi.org/10.7150/thno.11251

35. Rempel SA, Dudas S, Ge S, et al. Identification and localization of the cytokine SDF1 and its receptor, CXC chemokine receptor 4, to regions of necrosis and angiogenesis in human glioblastoma. Clin Cancer Res 2000; 6:102–111.
36. Zhou W, Jiang Z, Song X, et al. Promoter hypermethylation-mediated down-regulation of CXCL12 in human astrocytoma. J Neurosci Res 2008; 86:3002–3010. https://doi.org/10.1002/jnr.21746
37. Barbero S, Bonavia R, Bajetto A, et al. Stromal cell-derived factor 1α stimulates human glioblastoma cell growth through the activation of both extracellular signal-regulated kinases 1/2 and Akt. Cancer Res 2003; 63:1969–1974.
38. Lange F, Kaemmerer D, Behnke-Mursch J, et al. Differential somatostatin, CXCR4 chemokine and endothelin A receptor expression in WHO grade I-IV astrocytic brain tumors. J Cancer Res Clin Oncol 2018; 144:1227–1237. https://doi.org/10.1007/s00432-018-2645-1
39. Ma X, Shang F, Zhu W, et al. CXCR4 expression varies significantly among different subtypes of glioblastoma multiforme (GBM) and its low expression or hypermethylation might predict favorable overall survival. Expert Rev Neurother 2017; 17:941–946. https://doi.org/10.1080/14737175.2017.1351299
40. Stevenson CB, Ehtesham M, McMillan KM, et al. CXCR4 expression is elevated in glioblastoma multiforme and correlates with an increase in intensity and extent of peritumoral T2-weighted magnetic resonance imaging signal abnormalities. Neurosurgery 2008; 63:560. https://doi.org/10.1227/01.NEU.0000324896.26088.EF
41. Woerner BM, Warrington NM, Kung AL, et al. Widespread CXCR4 activation in astrocytomas revealed by phospho-CXCR4-specific antibodies. Cancer Res 2005; 65:11392–11399. https://doi.org/10.1158/0008-5472.CAN-05-0847
42. Isci D, D'Uonnolo G, Wantz M, et al. Patient-oriented perspective on chemokine receptor expression and function in glioma. Cancers 2021; 14:130. https://doi.org/10.3390/cancers14010130
43. Jones W, Griffiths K, Barata PC, et al. PSMA theranostics: review of the current status of PSMA-targeted imaging and radioligand therapy. Cancers 2020; 12:1367. https://doi.org/10.3390/cancers12061367
44. Lapa C, Lückerath K, Kleinlein I, et al. 68Ga-pentixafor-PET/CT for imaging of chemokine receptor 4 expression in glioblastoma. Theranostics 2016; 6:428. https://doi.org/10.7150/thno.13986
45. Wen PY, Macdonald DR, Reardon DA, et al. Updated response assessment criteria for high-grade gliomas: response assessment in neuro-oncology working group. J Clin Oncol 2010; 28:1963–1972. https://doi.org/10.1200/JCO.2009.26.3541
46. Zhu M, Han F, Gao J, et al. Clinically available and reproducible prediction models for IDH and CDKN2A/B gene status in adult-type diffuse gliomas. Acad Radiol 2024. https://doi.org/10.1016/j.acra.2024.06.020
47. Sun C, Jiang C, Wang X, et al. MR-based radiomics predicts CDK6 expression and prognostic value in high-grade glioma. Acad Radiol 2024; 31:5164–5174. https://doi.org/10.1016/j.acra.2024.06.006
48. Lv S, Sun B, Zhong X, et al. The clinical implications of chemokine receptor CXCR4 in grade and prognosis of glioma patients: a meta-analysis. Mol Neurobiol 2015; 52:555–561. https://doi.org/10.1007/s12035-014-8894-3
49. Tabouret E, Tchoghandjian A, Denicolai E, et al. Recurrence of glioblastoma after radio-chemotherapy is associated with an angiogenic switch to the CXCL12-CXCR4 pathway. Oncotarget 2015; 6:11664. https://doi.org/10.18632/oncotarget.3256
50. Jacobs SM, Wesseling P, de Keizer B, et al. CXCR4 expression in glioblastoma tissue and the potential for PET imaging and treatment with [(68)Ga]Ga-Pentixafor /[(177)Lu]Lu-Pentixather. Eur J Nucl Med Mol Imaging 2022; 49:481–491. https://doi.org/10.1007/s00259-021-05196-4
51. Komatani H, Sugita Y, Arakawa F, et al. Expression of CXCL12 on pseudopalisading cells and proliferating microvessels in glioblastomas: an accelerated growth factor in glioblastomas. Int J Oncol 2009; 34:665–672. https://doi.org/10.3892/ijo_00000192
52. Wang Z, Zhang M, Wang L, et al. Prospective study of (68)Ga-NOTA-NFB: radiation dosimetry in healthy volunteers and first application in glioma patients. Theranostics 2015; 5:882–889. https://doi.org/10.7150/thno.12303
53. Kaemmerer D, Trager T, Hoffmeister M, et al. Inverse expression of somatostatin and CXCR4 chemokine receptors in gastroenteropancreatic neuroendocrine neoplasms of different malignancy. Oncotarget 2015; 6:27566–27579. https://doi.org/10.18632/oncotarget.4491
54. Gravina GL, Mancini A, Colapietro A, et al. The novel CXCR4 antagonist, PRX177561, reduces tumor cell proliferation and accelerates cancer stem cell differentiation in glioblastoma preclinical models. 1010428317695528 Tumour Biol 2017; 39. https://doi.org/10.1177/1010428317695528
55. Bianco AM, Uno M, Oba-Shinjo SM, et al. CXCR7 and CXCR4 expressions in infiltrative astrocytomas and their interactions with HIF1α expression and IDH1 mutation. Pathol Oncol Res 2015; 21:229–240. https://doi.org/10.1007/s12253-014-9813-7
56. Demmer O, Dijkgraaf I, Schumacher U, et al. Design, synthesis, and functionalization of dimeric peptides targeting chemokine receptor CXCR4. J Med Chem 2011; 54:7648–7662. https://doi.org/10.1021/jm2009716
57. Lapa C, Knop S, Schirbel A, et al. First in man experience of CXCR4-directed endoradiotherapy with 177Lu-and 90Y-labelled Pentixather in multiple myeloma patients. Soc Nuclear Med 2015; 57:248–251.
58. Liu SC, Alomran R, Chernikova SB, et al. Blockade of SDF-1 after irradiation inhibits tumor recurrences of autochthonous brain tumors in rats. Neuro Oncol 2014; 16:21–28. https://doi.org/10.1093/neuonc/not149
59. Redjal N, Chan JA, Segal RA, et al. CXCR4 inhibition synergizes with cytotoxic chemotherapy in gliomas. Clin Cancer Res 2006; 12:6765–6771. https://doi.org/10.1158/1078-0432.CCR-06-1372